Waves and related processes in Geophysical Fluid Dynamics

V. Zeitlin

Laboratoire de Météorologie Dynamique, Sorbonne University and École Normale Supérieure, Paris

Waves in Flows, Prague, August 2018

Plan

Linear (in)stability, reminder

Instability and hybrid modes : example of coastal currents

Baroclinic and barotropic instabilities of atmospheric and oceanic jets

- Geostrophic instabilities
- Ageostrophic instabilities

Trapped-waves origin of inertial instability

Résumé

Stable and unstable waves

Previously :

Linearisation about state of rest $\rightarrow$ Fourier-transform in time and space $\rightarrow$ algebraic eigen system for time frequencies ω (easy !) $\rightarrow$ solvability condition $\rightarrow$ wave spectrum.
Wave spectrum $\leftrightarrow$ dispersion relation $\omega = \omega(\boldsymbol{k})$ with real eigenfrequencies.

Generally :

Linearisation about a stationary state $\rightarrow$ Fourier-transform in time $\rightarrow$ eigen system of linear PDE for frequencies in space (not easy !).
Specific solutions : jets and vortices (translationally, resp. azimuthally symmetric) $\Rightarrow$ partial Fourier-transform in space. Simple, or no vertical structure : eigen system of linear ODE for frequencies in one spatial variable (easy again !). But the spectrum, in general, is complex : $\omega = \omega_r \pm i\sigma \Rightarrow$ instability, with growth rate σ.

Stability diagram of the coastal current in 1-layer RSW

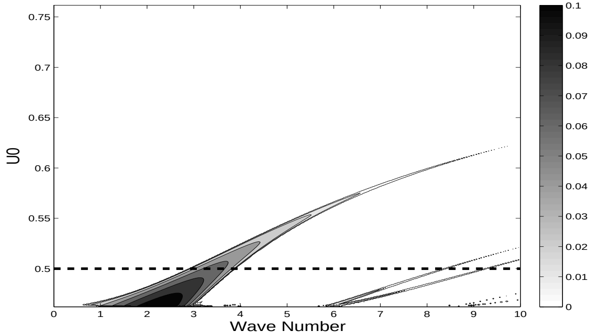

Levels of gray : growth rates.

Dispersion diagram in the stable region

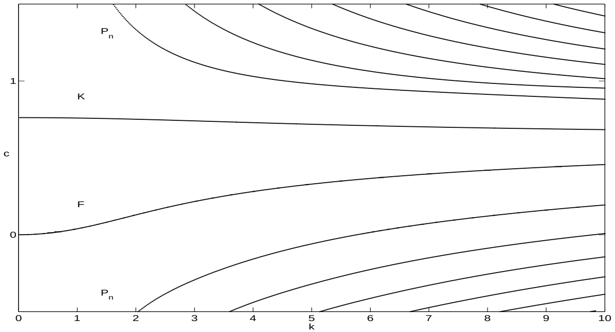

Phase velocity as a function of wavenumber.

Dispersion diagram in the unstable region

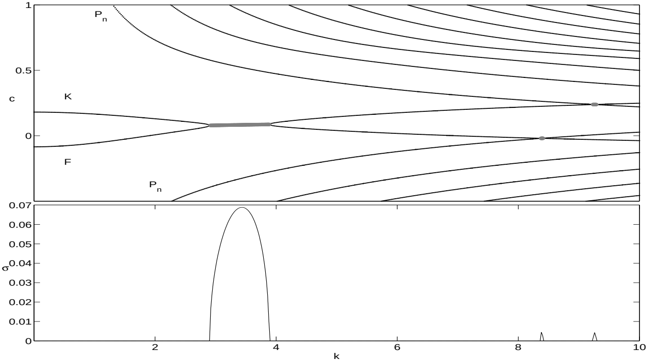

Upper panel : dispersion relation. Lower panel : growth rates.

Phase portrait of the unstable KF mode

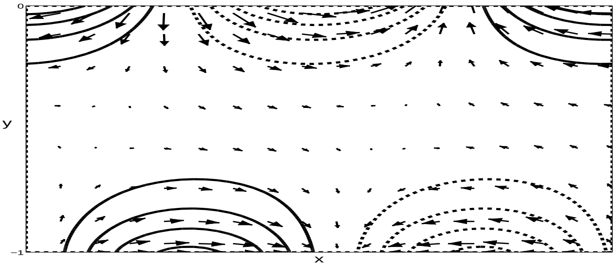

Unstable mode corresponding to the intersection of dispersion curves of Kelvin and Frontal waves.
Remark : identification of unstable modes as intersections of dispersion curves is sure in (piece-wise)constant PV flows ; complications in the presence of critical layers.

Could be worse...

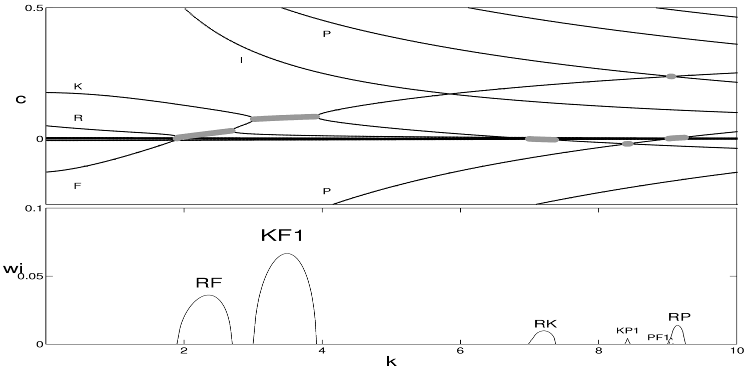

Dispersion and stability diagrams for an upper-layer coastal current in the 2-layer RSW. Depth ratio 10.

Phillips model in the f- plane approximation

2-layer QG model considered in the limit $\frac{\rho_2-\rho_1}{\rho_2} \to 0$, and hence $\eta \to \pi_2 - \pi_1$:

$$\frac{d_i^{(0)}}{dt}\left[\nabla^2\pi_i - (-1)^i F_i\,\eta\right] = 0\,,\;\; i = 1,2, \qquad (1)$$

$F_i = D_i^{-1} = \text{const.}$
An exact solution of these equations is a zonal flow in geostrophic equilibrium : $U_i = \partial_y \pi_i$, $i = 1, 2$. If $U_1 \neq U_2$ the flow has a vertical shear corresponding to the inclined interface : $\eta = \pi_2 - \pi_1 = (U_1 - U_2)y$. Linearisation about the background flow

$$\pi_i = -U_i y + \phi_i, \quad ||\phi|| \ll 1, \to$$

$$(\partial_t + U_i\partial_x)\left[\vec{\nabla}^2\phi_i - (-1)^i F_i(\phi_2 - \phi_1)\right] - \left[(-1)^i F_i(U_1 - U_2)\right]\partial_x\phi_i = 0. \qquad (2)$$

Sketch of the Phillips model

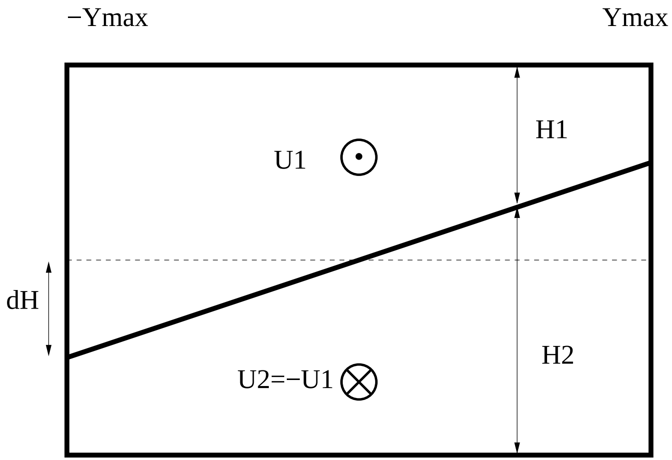

Dispersion relation

Wave solutions : $\phi_i = A_i e^{i(\mathbf{k}\cdot\mathbf{x}-\omega t)} + c.c.$, phase-speed $c = \omega/k_x$, $U_1 - U_2 = \Delta U$, $\rightarrow$

$$\begin{cases} A_1 \left[(c-U_1)(\mathbf{k}^2+F_1)+F_1(U_1-U_2)\right] - A_2(c-U_1)F_1 = 0, \\ -A_1(c-U_2)F_2 + A_2\left[(c-U_2)(\mathbf{k}^2+F_2)-F_2(U_1-U_2)\right]. \end{cases} \tag{3}$$

Dispersion relation :

$$\begin{aligned} c &= \frac{1}{2(\mathbf{k}^2+F_1+F_2)}\Big[U_1(\mathbf{k}^2+2F_2)+U_2(\mathbf{k}^2+2F_1) \\ &\pm \left[(\Delta U)^2\left(\mathbf{k}^4-4F_1F_2\right)\right]^{\frac{1}{2}}\Big]. \end{aligned} \tag{4}$$

Classical baroclinic long-wave instability

Upper-layer Bickley jet in the *f*- plane

$$U_1 = 0, \quad \bar{\eta}_1 = \frac{1}{\alpha - 1}\tanh(y),$$

$$U_2 = \mathrm{sech}^2(y), \quad \bar{\eta}_2 = \frac{-1}{\alpha - 1}\tanh(y). \qquad (5)$$

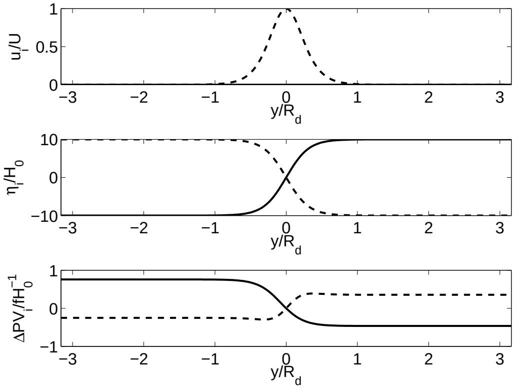

$Ro = 0.1$ Lower (upper) layer : solid (dashed).

Stability diagram and most unstable mode

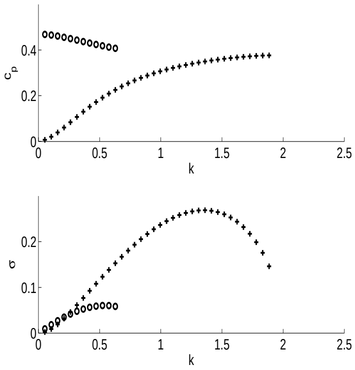

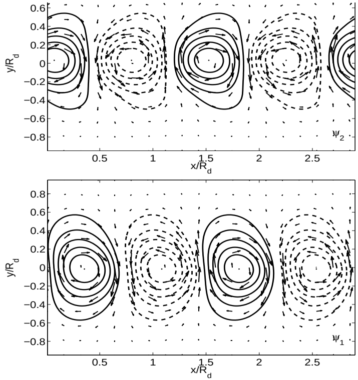

Left : Linear stability diagram of the upper-layer Bickley jet : phase velocity (top) and growth rate (bottom). *Right :* The most unstable mode . Positive (solid) and negative (dashed) pressure anomalies (contours) and velocities (arrows) in the upper (top) and lower (bottom) layers.

Nonlinear saturation of the baroclinic instability

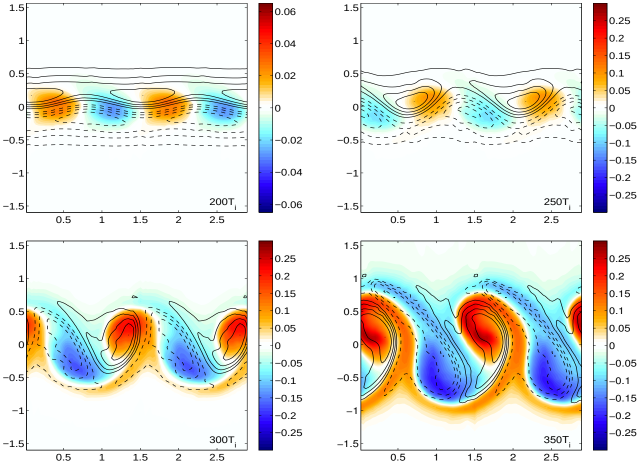

Relative vorticity in lower (colours) and upper (contours) layers.

Baroclinic instability in Nature

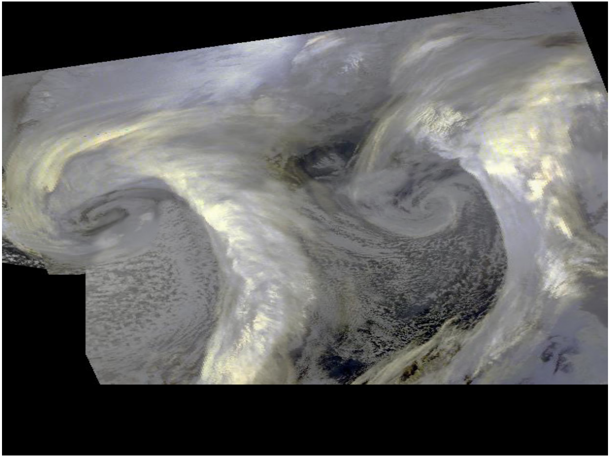

Satellite view of a couple of synoptic disturbances over the North Atlantic.

Ageostrophic Phillips model

Stationary state : geostrophic equilibrium layer-wise :

$$U_j(y) = -\frac{1}{\rho_j f}\partial_y \Pi_j,\ j = 1, 2, \tag{6}$$

where Π_j is pressure in the layer j. Phillips model : U_j are constant, and $H_j(y)$, the unperturbed thicknesses, are linear in y. Small perturbations :
$h_j = H_j(y) + (-1)^j \eta(x, y, t),\ \pi_j \to \Pi_j(y) + \pi_j(x, y, t)$,
linearisation and non-dimensionalisation :

$$\begin{cases} \partial_t u_j + FU_j \partial_x u_j - v_j = \frac{1}{\rho_j}\partial_x \pi_j, \\ \partial_t v_j + FU_j \partial_x v_j + u_j = \frac{1}{\rho_j}\partial_y \pi_j, \\ \partial_t \eta + FU_j \partial_x \eta = (-1)^{j+1} F \left(H_j \partial_x u_j + \partial_y (H_j v_j)\right), \\ \pi_2 - \pi_1 = \frac{2}{F}\eta. \end{cases} \tag{7}$$

Froude number $F = \frac{U_0}{\sqrt{gH}} = \frac{U_0}{fR_d}$ is synonymous to the Rossby number, as all distances are scaled with the baroclinic deformation radius R_d

Stability diagram in ageostrophic Phillips model

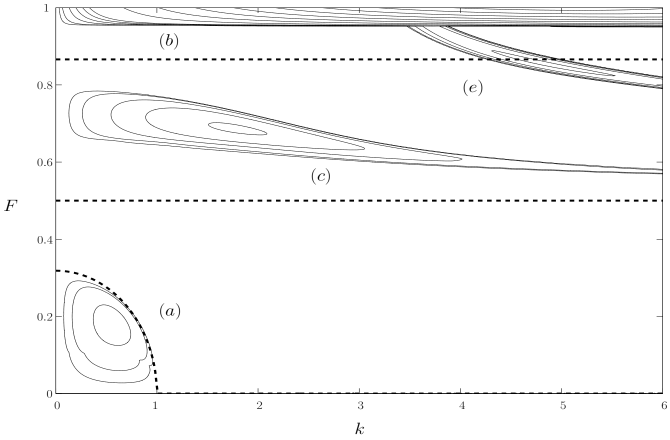

Dispersion and growth rates in ageostrophic Phillips model

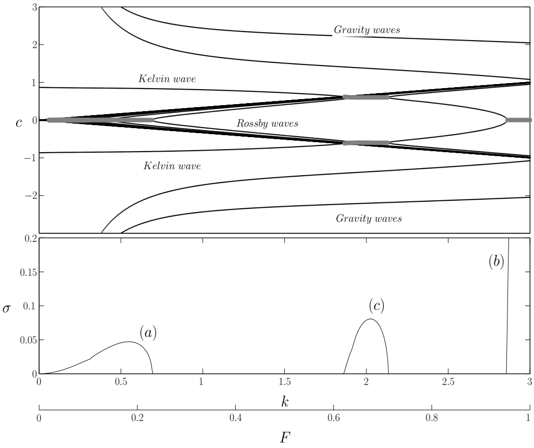

Unstable Rossby-Kelvin wave

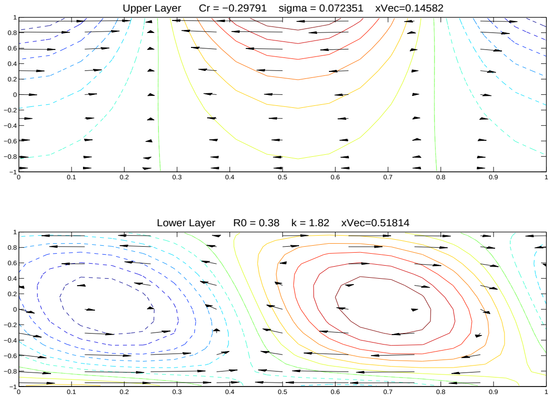

Barotropic Bickley jet with $Ro = 5$ in 2-layer model

$$H_1(x) = H_{10},\ H_2(x) = H_{20} + \delta \tanh\left(\frac{x}{L}\right), \qquad (8)$$

$$U_{1,2}(x) = 0,\ V_{1,2}(x) = \frac{g\delta}{fL}\left(1 - \tanh^2\left(\frac{x}{L}\right)\right). \qquad (9)$$

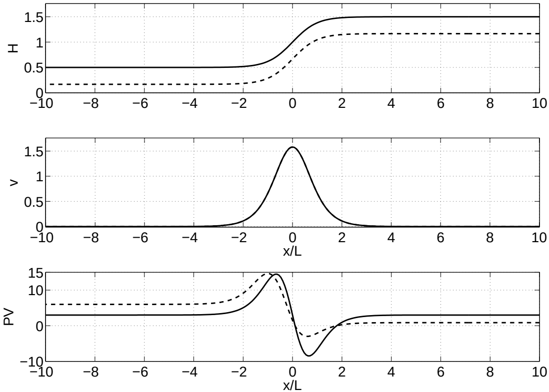

Stability diagram at small *Ro*

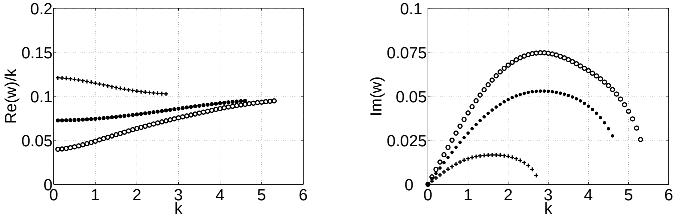

Left panel : phase velocity $Re(\omega)/k$.
Right panel : growth rate $Im(\omega)$, as functions of k for unstable modes of a quasi-geostrophic jet with $Ro = 0.5$.

The most unstable mode at small *Ro*

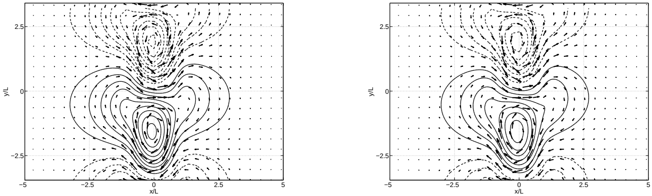

Structure of the most unstable mode with $k = 2.85$, $Im(\omega) = 0.075$, $Re(\omega)/k = 0.073$ of the upper branch. *Left (Right) panel* : upper (lower) layer. Pressure (contours) and velocity (arrows) anomaly.

The second unstable mode at small *Ro*

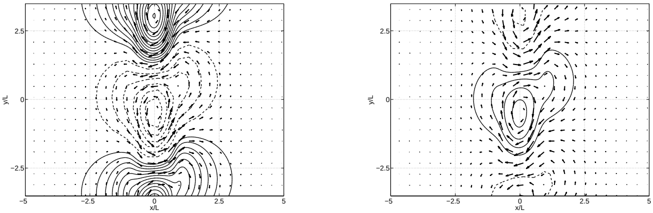

Structure of the most unstable mode with $k = 2.8$, $Im(\omega) = 0.05$, $Re(\omega)/k = 0.085$ of the middle branch . *Left (Right) panel* : upper (lower) layer. Pressure (contours) and velocity (arrows) anomaly.

The third unstable mode at small *Ro*

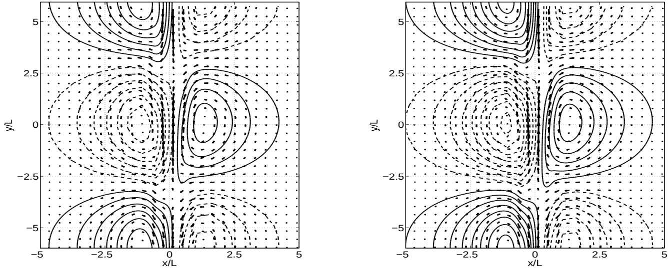

Structure of the most unstable mode with $k = 1.65$, $Im(\omega) = 0.016$, $Re(\omega)/k = 0.073$ on the lower branch. *Left (Right) panel* : upper (lower) layer. Pressure (contours) and velocity (arrows) anomaly.

Stability diagram at large *Ro*

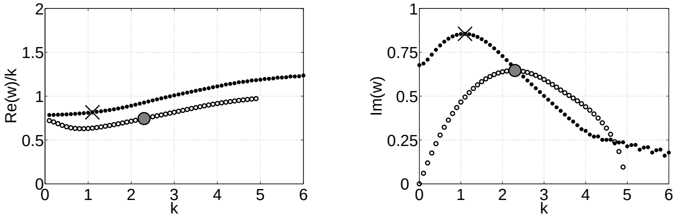

Left : phase velocity $Re(\omega)/k$ and *Right :* growth rate $Im(\omega)$ as functions of k for the unstable modes of a strongly ageostrophic jet with $Ro = 5$. Translationally symmetric instability appears at $k = 0$: inertial instability.

The most unstable mode at large *Ro*

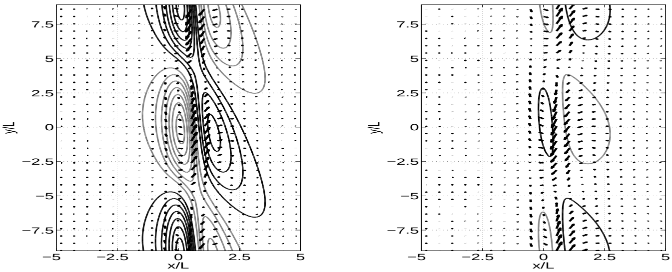

Structure of the most unstable mode with $k = 1.1$, $Im(\omega) = 0.86$, $Re(\omega)/k = 0.82$ of the jet with $Ro = 5$. *Left (Right) panel :* Pressure (contours) and velocity (arrows) anomaly in *upper (lower) layer*.

A clearly baroclinic mode

The second unstable mode at large *Ro*

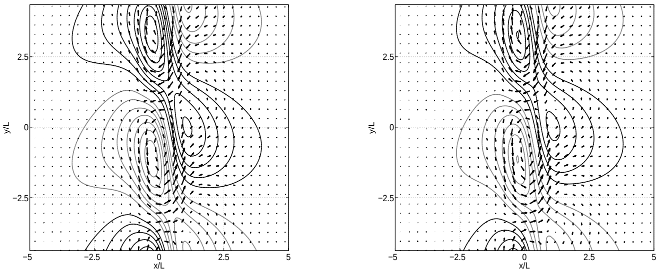

Structure of the most unstable mode with $k = 2.25$, $Im(\omega) = 0.65$, $Re(\omega)/k = 0.75$of the jet with $Ro = 5, d = 2$. *Left (Right) panel :* Pressure (contours) and velocity (arrows) anomaly in *upper (lower) layer*.

A clearly barotropic mode - swap of instabilities

Span-wise structure of inertial instability

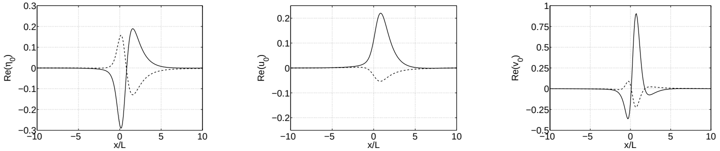

Cross-section of the translationally symmetric unstable mode with $k = 0$. *Dashed :* layer 2 ; *solid :* layer 1. From left to right : amplitudes of the interface deviation, cross-stream and streamwise velocities.

Translationally-invariant 2-layer RSW

$$\begin{cases} \partial_t u_1 + u_1 \partial_x u_1 - f v_1 + \rho_1^{-1} \partial_x \pi = 0 \ , \\ \partial_t v_1 + u_1 (f + \partial_x v_1) = 0 \ , \\ \partial_t u_2 + u_2 \partial_x u_2 - f v_2 + \rho_2^{-1} \partial_x \pi + g' \partial_x \eta = 0 \ , \\ \partial_t v_2 + u_2 (f + \partial_x v_2) = 0 \ , \\ \partial_t (H_1 - \eta) + \partial_x ((H_1 - \eta) u_1) = 0 \ , \\ \partial_t (H_2 + \eta) + \partial_x ((H_2 + \eta) u_2) = 0 \ , \end{cases} \tag{10}$$

where $(u_1,\ v_1)$, $(u_2,\ v_2)$ are velocity components in the upper and lower layer, respectively ; π is barotropic pressure ; η is displacement of the interface, H_1 and H_2 are thicknesses of the layers at rest ;
$H = H_1 + H_2 = const$, g' is the reduced gravity :
$g' = g(\rho_2 - \rho_1)/\rho_2$.

Linearisation about geostrophic equilibrium

Geostrophic equilibria

$$v_1 = \frac{1}{f\,\rho_1}\,\partial_x \pi\ , \quad v_2 = \frac{1}{f \rho_2}\,\partial_x \pi + \frac{g'}{f}\partial_x \eta\ . \qquad (11)$$

Non-dimensional expressions :

$$V_{1g} = \partial_x \Pi\ , \quad V_{2g} = r\,\partial_x \Pi + Bu\,\partial_x h_{2g}\ , \qquad (12)$$

$r = \frac{\rho_1}{\rho_2}$, $Bu = \frac{g'\,H_2}{f^2 L^2}$. Localised jets : velocity rapidly decaying with $|x|$.

Linearisation about a state of geostrophic equilibrium :

$$\begin{cases} \partial_t u_1 - v_1 + \partial_x \Pi = 0\ , \\ \partial_t v_1 + u_1(1 + \partial_x V_{1g}) = 0\ , \\ \partial_t u_2 - v_2 + r\partial_x \Pi + Bu\partial_x \eta = 0\ , \\ \partial_t v_2 + u_2(1 + \partial_x V_{2g}) = 0\ , \\ \partial_t \eta - \partial_x(h_{1g} u_1) = 0\ , \\ \partial_t \eta + \partial_x(h_{2g} u_2) = 0\ . \end{cases} \qquad (13)$$

Reduction to a single equation

New variable : $U = h_{2g} u_2 = -h_{1g} u_1$, single equation :

$$Bu\, \partial^2_{xx} U - \left[\frac{r h_{2g} + h_{1g}}{h_{1g} h_{2g}} (\partial^2_{tt} + 1) + \frac{r\, \partial^2_{xx} \Pi}{h_{1g} h_{2g}} + Bu\, \frac{\partial^2_{xx} h_{2g}}{h_{2g}} \right] U = 0 . \tag{14}$$

Notation :

$$F(x) = \frac{r h_{2g} + h_{1g}}{h_{1g} h_{2g}} , \quad G(x) = \frac{r\, \partial^2_{xx} \Pi}{h_{1g} h_{2g}} + Bu\, \frac{\partial^2_{xx} h_{2g}}{h_{2g}} , \tag{15}$$

Fourier-transformation $U(x,t) = \int d\omega \tilde{U}(\omega, x) e^{-i\omega t} + c.c.$

$$Bu\, \partial^2_{xx} \tilde{U} - \left(F(1 - \omega^2) + G \right) \tilde{U} = 0 . \tag{16}$$

Instability

Integral estimate

Multiplication by $\tilde{U}^*$ and integration in x, assuming localised = trapped solutions :

$$\omega^2 = 1 + \frac{Bu \int |\partial_x \tilde{U}|^2 \, dx + \int G|U|^2 \, dx}{\int F|\tilde{U}|^2 \, dx} \, . \tag{17}$$

content...

Analysis

F positive, but G can be negative, in anticyclonic regions where $\partial^2_{xx}\Pi < 0$. Strong enough anticyclonic shears $\Rightarrow$ $\omega^2 < 1$, and can even become negative $\Leftrightarrow$ instability.

Illustration/interpretation

For a jet with flat interface $\eta = 0 \Leftrightarrow h_g = \text{const}$:

$$Bu\, \partial^2_{xx} U - \left[(\partial^2_{tt} + 1)\, H_e^{-1} + r\partial^2_{xx}\Pi\, (H_1 H_2)^{-1} \right] U = 0 \,. \tag{18}$$

After Fourier-transformation in time we get $\left(H_e = \frac{H_1 H_2}{H_1 + H_2} \right)$:

$$\partial^2_{xx} \tilde{U} + \frac{1}{Bu} \left[\omega^2 H_e^{-1} - (H_e^{-1} + (H_1 H_2)^{-1} r\partial^2_{xx}\Pi) \right] \tilde{U} = 0 \,. \tag{19}$$

Shrödinger equation of quantum mechanics :

$$\partial^2_{xx}\psi + (E - V(x))\psi = 0 \tag{20}$$

for a particle with energy $E = \omega^2 (H_e\, Bu)^{-1}$ moving in the potential $V(x) = Bu^{-1}\, (H_e^{-1} + (H_1 H_2)^{-1} r\partial^2_{xx}\Pi)$. Potential well deep enough : particle trapped. For deep potential wells, nothing prevents the eigenvalues of "energy" to become negative $\Leftrightarrow$ purely imaginary ω.

What have we seen :

- Waves propagating on the background of a mean flow can phase-lock, forming hybride waves, and grow
- Classical baroclinic instability can be explained in this way
- Jet instabilities undergo a "phase transition" with increasing Rossby number, with appearance of translationally invariant inertial instability
- Inertial instability is due to trapped in the anticyclonic shear waves

What we have not seen :

Nonlinear interactions of waves - coming up !